Petrogenesis of monzonoritic dykes in the Egersund-Ogna anorthosite (Rogaland, S.W. Norway): trace elements and isotopic (Sr, Pb) constraints

J.C. Duchesne[1], I. Roelandts[1], D. Demaiffe[2], and D. Weis[2] *

[1] Laboratoires associés de Géologie, Pétrologie, Géochimie, Université de Liège, B-4000 Sart Tilman, Belgium
[2] Laboratoires associés de Géologie-Pétrologie-Géochronologie, Université Libre de Bruxelles, 50, avenue Fr. Roosevelt, B-1050 Bruxelles, Belgium

Abstract. Two major monzonoritic dykes occur in the Egersund-Ogna anorthositic massif (S.W. Norway): the Lomland dyke, which varies from norite to monzonite, and the Vettaland ferronoritic dyke. They are characterized by high Fe, Ti and P contents, low SiO_2, variable K_2O (0.5%–4.5%) and high Fe/Mg ratios. Small variations in REE distribution are observed inside the Lomland dyke [La/Yb = 12; LREE ca. 150–180 (chondrite-normalized values), neutral to slightly positive Eu anomaly]. Part of the Vettaland dyke is severely depleted in Zr, Rb and REE and shows a positive Eu anomaly. All rocks are depleted in U and Th, and show very low Cr and Ni contents, as well as high Sr contents (400–600 ppm).

Variation within the Lomland dyke is satisfactorily explained through subtraction of an apatite-bearing noritic cumulate. The role of apatite is predominant in controlling the REE behaviour. Eutectic partial melting of a Fe-rich noritic cumulate (containing apatite) under low pH_2O conditions is suggested for the Vettaland dyke by REE modelling.

Sr isotopic initial ratios are different in Lomland (ca. 0.708) and Vettaland (ca. 0.706) dykes. These values preclude direct derivation from the mantle as well as comagmatic relationship with anorthosite. Contamination of a mantle derived magma by deep crustal material or anatexis of the LIL depleted lower crust is compatible with the low U and Th contents, and with the Pb isotopic ratios. The Vettaland partial melting process is extended to all monzonoritic types, the necessary heat being provided by the high temperature anorthositic crystal mush.

Introduction

Monzonoritic[a] rocks form dykes and small intrusions in massif-type anorthosites (Emslie 1978). Though much smaller in volume than the associated acidic rocks, they are ubiquitous in all anorthositic provinces. They frequently intrude the contact between anorthositic massifs and their

---

[a] Monzonorite stands for hypersthene monzogabbro/monzodiorite, or jotunite. It is extended here to ferrodiorite, ferronorite and to quartz-bearing varieties

* Chargé de Recherches du F.N.R.S (Belgium)

Offprint requests to: J.C. Duchesne

envelope of metamorphic gneisses. They belong to the anorthosite-quartz mangerite (charnockite) suite of rocks.

Various hypotheses have been proposed for the genesis of monzonoritic rocks. They have been interpreted as comagmatic with the anorthosites (Buddington 1972; Ashwal 1982; Wiebe 1984). Whatever the composition of the parental magma, plagioclase fractionation tends to enrich the liquid in, for example Fe, Ti and P. The overall similarity of monzonorites with Skaergaard ferrodiorites (Wager and Brown 1968) is in agreement with this hypothesis.

For Michot (1960, 1965) and Philpotts (1966), the consanguinity between monzonorites and anorthosites is extended to the whole anorthosite suite. The monzonorites were thought to represent liquids of intermediate composition in a continuous evolution by fractional crystallization from anorthosites to quartz mangerites.

Discovery in the Hidra body (S.W. Norway) of a contact facies (Duchesne et al. 1974) of monzonoritic composition showing no Eu anomaly has, however, questioned the residual character of the monzonorites. Indeed, a magmatic liquid left after fractionation and subtraction of an important quantity of plagioclase should display a significant negative Eu anomaly, as well as a Sr depletion. The absence of Eu anomaly and the high Sr content of monzonorite (400–600 ppm) thus preclude a residual character for this rock.

These geochemical studies gave rise to two contrasting views on the status of monzonorites in anorthositic magmatism. On the one hand, Duchesne and Demaiffe (1978) suggested monzonoritic liquid was the parental magma of the andesine anorthosites. Trace element modelling of the Bjerkreim-Sokndal sequence of rocks (Duchesne 1978; Roelandts and Duchesne 1979) and of the Hidra body (Demaiffe and Hertogen 1981) gave results compatible with this hypothesis. On the other hand, Emslie (1978) considered that monzonorites (ferrodiorites) represent late-stage products of olivine- and orthopyroxene-fractionation from a tholeiitic magma in a sub-crustal chamber before intrusion in the anorthosite massifs. Emslie admits some decoupling between the production of anorthosites and that of monzonorites. Another interpretation has been made by Philpotts (1981), who considered that monzonoritic liquids could have been produced by immiscibility and were conjugate to quartz mangeritic liquids.

The purpose of the present study is to provide additional data on monzonorites occurring in the Egersund province,
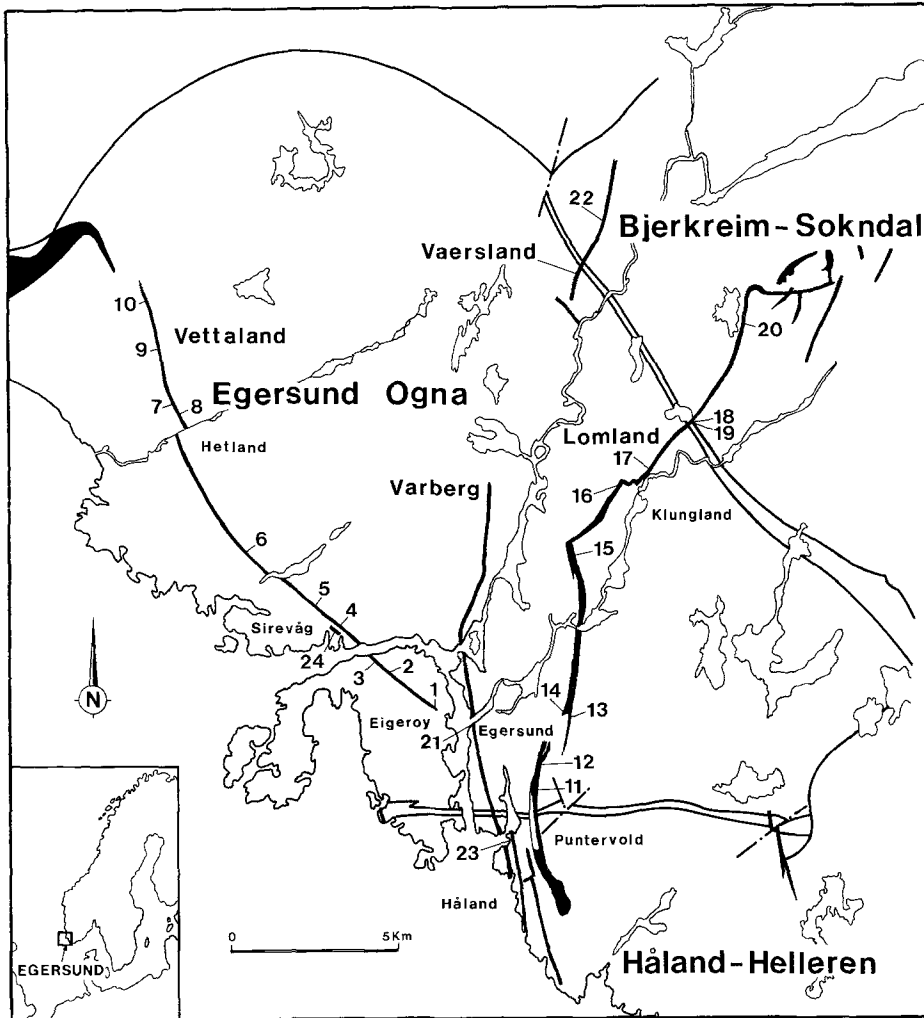
and to see what light these data can throw on the petrogenesis of these rocks.

Geological framework and petrography

Monzonoritic rocks occur in numerous dykes and small intrusions in the Rogaland anorthositic province (S.W. Norway) (Michot and Michot 1969; Duchesne et al. 1984). They were emplaced around 950 Ma (Pasteels et al. 1979), near the end of the igneous event and clearly intrude after the granulite facies regional metamorphism (Weis and Demaiffe 1983b; Demaiffe and Michot 1985).

Several monzonoritic dykes (Fig. 1), which cut across the Egersund-Ogna massif-type anorthosite and its neighbouring massifs – the Håland massif and the Bjerkreim-Sokndal lopolith – are studied here with special attention to the Vettaland (samples 1–10) and the Lomland (samples 11–20) dykes (Michot 1960), which extend over more than 20 km and have an average thickness of several tens of metres. The Varberg (no. 21), Vaersland (no. 22), Håland (no. 23) and Sirevåg (no. 24) dykes were also sampled.

The Lomland dyke. This major dyke shows a continuous variation from an antiperthitic norite (Puntervold facies) in the south to a monzonorite/monzonite (Klungland facies) in the north. The

antiperthitic norites are massive medium-grained rocks (5–10 mm) of subophitic texture (samples 11–14). Plagioclase is euhedral, tabular (An_{40}, slightly zoned) and contains antiperthite blebs. Large poikilitic crystals (up to 1 cm) of inverted pigeonite develop between the plagioclases. Homogeneous ilmenite and Ti-poor magnetite fill the interstices between all minerals. Apatite is relatively abundant.

The monzonorites and monzonites (samples 16–20) are characterized by tabular mesoperthite-mantled plagioclase in a mesostasis (500 μm) of plagioclase and micro- to mesoperthitic K-feldspar in subequal amounts, variable amounts of quartz, large poikilitic inverted pigeonite, clinopyroxene, apatite, zircon and oxide minerals (homogeneous ilmenite and Ti-magnetite). A continuous gradation exists between the Puntervold and the Klungland facies through increase in K-feldspar and quartz contents and the development of the mesostasis.

The Vettaland dyke. This differs from the Lomland dyke by its texture and composition. In its southern part (Eigerøy facies) (samples 1–6), the rock is an antiperthitic norite with or without quartz. The texture is equigranular, composed of a regular mosaic of anhedral antiperthitic plagioclase, quartz, inverted pigeonite, subordinate clinopyroxene, homogeneous ilmenite, Ti-magnetite and traces of pyrrhotite. From Hellvik to the North (Hetland facies), the rock (samples 7–10) contains some antiperthitic plagioclase slightly coarser than the average mosaic. This feature neither modifies the major element composition of the rock, which is remarkably constant in the whole dyke (see below), nor increases the Sr content relative to the Eigerøy facies.

Table 1. Major and some trace element composition

	Vettaland		Lomland			Var[b] 21 7520	Vaers 22 66192	Hald 23 7548	Sirev 24 75542
	mean n=10	s	P[a]	15 7553	K[b]				
SiO$_2$	49.9	2.75	43.88	47.29	51.60	46.33	55.82	58.78	52.02
TiO$_2$	2.7	0.35	4.45	3.56	2.41	3.62	2.24	2.19	2.14
Al$_2$O$_3$	13.1	0.71	12.89	13.34	14.65	12.68	13.39	13.52	15.04
Fe$_3$O$_3$	4.1	0.47	5.13	4.08	4.90	4.84	3.27	3.43	4.38
FeO	14.7	1.56	13.20	12.62	8.87	13.45	9.70	7.41	9.64
MnO	0.27	0.03	0.26	0.27	0.19	0.25	0.19	0.17	0.23
MgO	2.40	0.39	3.94	3.58	2.26	3.27	1.96	1.97	2.14
CaO	7.5	0.76	8.76	7.65	6.21	7.63	5.20	4.88	6.21
Na$_2$O	2.9	0.18	3.26	3.59	3.96	3.33	3.24	3.72	4.05
K$_2$O	0.78	0.23	1.02	1.76	3.00	1.76	3.60	3.11	2.69
P$_2$O$_5$	1.66	0.33	2.99	2.18	1.44	2.47	1.30	1.11	1.01
Total	100.01		99.77	99.92	99.49	99.62	99.91	100.29	99.55

Normative composition (wt %)

Or	4.6	1.3	6.0	10.4	17.8	10.4	21.3	18.3	14.9
Ab	24.3	1.4	27.6	30.4	33.6	28.2	27.4	31.3	34.1
An	20.5	1.6	17.5	15.1	13.4	14.5	11.3	10.9	12.0
Q	7.2	3.5	–	–	2.1	0.3	8.6	12.7	0.1
Cpx	6.1	0.7	7.1	8.5	7.6	7.6	5.8	5.6	9.7
Opx	22.5	3.0	18.7	15.6	10.5	19.6	13.7	9.5	16.3
Ol	–	–	0.6	2.6	–	–	–	–	–
Mt	5.9	0.7	7.5	5.9	7.1	7.0	4.7	5.0	6.4
Il	5.1	0.7	8.5	6.8	4.6	6.9	4.3	4.1	4.1
Ap	3.6	0.7	6.5	4.8	3.2	5.4	2.8	2.4	2.2

Trace elements (ppm)

	E[c]	H[d]							
Ba	485	699	720	1,451	1,800	1,064*	1,403*	1,747*	1,613*
Rb	<3**	5	5.3**	9.7	22	13.9	40	23.5	42
Sr	592	532	458**	417	393	406	294	335	347
Zr	30	1,185	55	89	572	215	867	770	1,591
Y	34	85	51	51	52	69	53	44	144
La	<15	45	40	37	44	58.7*	45*	47.2*	102*
Ce	32	131	112	98	103	149*	112*	110*	254*
Nd	27	91	72	68	67	88*	66*	67.6*	161*
Co	36	35	46	38	27	37*	21*	21*	21*
V	67	50	160	110	73	151	58	75	66
Zn	217	217	202	221	186	225	158	155	221
Ni	<10	<10	<10	<10	<10	<10	<10	<10	<10

* Determination by NAA (see Table 2)
** Determinations by isotope dilution
All other determinations by XRF (G. Bologne, analyst)

[a] P: Puntervold facies – average of samples 11–14 (66175; 7536; 7533; 7534)
[b] K: Klungland facies – average of samples 16–20 (7552; 72105; 7559; 7365; 8147)
[c] E: Eigeröy facies – average of analyses 1–6 (7613; 7611; 76123; 7555; 7557; 7522)
[d] H: Hetland facies – average of analyses 7–10 (7527; 75281; 75301; 7529)

The Varberg dyke is petrographically homogeneous: it is a monzonorite (sample 21) texturally similar to the Puntervold facies, but with more microperthitic feldspar. *The Vaersland dyke* (sample 22) is a quartz monzonite, petrographically homogeneous along strike. A particular facies has been sampled in the *Håland dyke*, south of Egersund (sample 23). It is a fine-grained quartz monzonite showing a granular texture (0.7 mm). Sample 24 (*Sirevåg*) is a fine-grained granular monzonorite from a thin dyke (1.5 m), which crops out not far from the Vettaland dyke, but with a clearly different chemical composition.

Geochemical data

Tables 1 and 2 give the major and trace element compositions (the methods are described in Appendix 2). The samples from the various petrographic facies are averaged in Table 1. Detailed analyses – which can be obtained from the authors – were used to plot Figs. 2–5. Results of NAA on selected samples are reported in Table 2 and Fig. 5.

The following chemical characteristics are observed for

Table 2. REE and other trace element composition (ppm)

| Rock	Vettaland			Lomland					Varb 21 7520	Vaers 22 66192	Hald 23 7548	Sirev 24 75542
	5 7557	6 7522	10 7529	11 66175	14 7534	16 7552	17 72105	18 7559				
La	6.31	6.81	51.0	42.4	39.7	42.6	37.8	45.9	58.7	44.8	47.2	102
Ce	18.3	21.0	130	109	99.3	109	91.6	106	149	112	110	254
Nd	19.0	21.2	90.2	72.7	69.2	67.6	60.4	66.6	88.0	66.2	67.6	161
Sm	7.12	8.12	25.7	20.1	17.8	18.1	15.6	15.9	23.4	17.2	15.9	38.5
Eu	4.93	5.06	7.97	6.82	6.77	7.51	7.69	7.38	7.81	6.49	5.69	7.22
Tb	0.94	1.16	3.54	2.39	2.15	2.34	1.90	1.99	2.85	2.15	1.88	5.29
Yb	1.72	1.91	4.51	2.78	2.48	3.13	2.75	3.15	4.73	3.71	3.51	13.1
Lu	0.25	0.32	0.65	0.43	0.35	0.50	0.39	0.47	0.74	0.57	0.54	2.08
Hf	2.80	11.6	6.05	2.57	2.99	9.06	8.27	13.3	5.32	18.1	17.4	39.4
Ta	<0.1	0.12	1.37	1.05	1.27	1.46	1.18	1.47	1.62	1.54	1.21	1.88
Sc	30.9	30.5	28.3	24.8	20.3	18.9	21.2	21.6	22.4	18.8	18.4	27.6
Cr	1.40	2.13	1.29	2.71	1.88	1.52	0.95	1.16	2.86	1.05	2.31	8.78
Co	33.0	31.3	32.6	51.4	39.9	27.3	26.8	26.2	37.1	20.6	20.7	20.7
Th	<0.2	<0.1	0.30	0.71	0.48	0.53	0.30	0.34	0.56	0.20	0.31	2.11
U	0.11	<0.1	0.26	0.31	0.28	0.18	0.16	0.31	0.30	0.20	0.24	0.53
Zr/Hf	25	37	48	22	28	49	45	48	40	48	44	40
Th/U			1.2	2.3	1.7	2.9	1.9	1.1	1.9	1.0	1.3	4.0
La/Yb	3.7	3.6	11.3	15.3	16.0	13.4	13.8	14.6	12.4	12.1	13.5	7.8
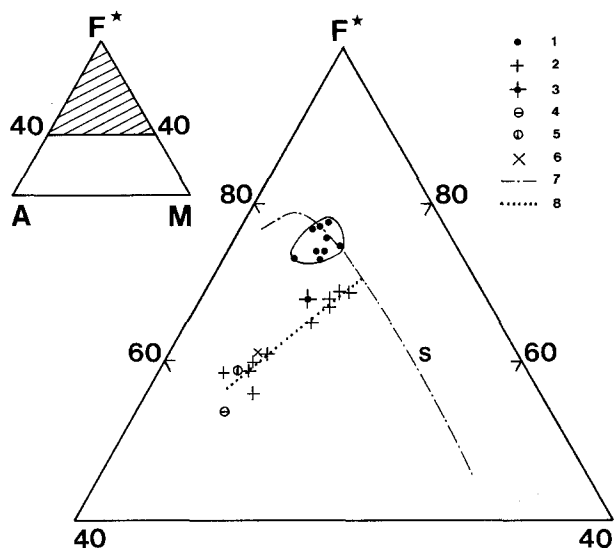
Fig. 2. $Na_2O + K_2O$ (A) – FeO* (F) – MgO (M) diagram. Legend: 1. Vettaland dyke; 2. Lomland dyke; 3. Varberg dyke; 4. Vaersland dyke; 5. Håland dyke; 6. Sirevåg dykelet; 7. evolution of the Skaergaard liquids (after Wager and Brown 1968); 8. evolution in the Lomland dyke

major elements: low SiO_2 contents (43–54%), high total Fe (11–20% FeO*), high TiO_2 (2–5%), high P_2O_5 (1–3.4%), K_2O between 0.5 and 4.5%, together with nearly constant and moderate Al_2O_3 (12–15%), low MgO (2–4%), high CaO (5–9%). The FeO*/MgO + FeO* ratios (Fig. 2) range from 0.80 to 0.90; K_2O is less than Na_2O; the norm indicates compositions near the limit of SiO_2 saturation. The Peacock index divides the rocks into two different groups: (1) the Vettaland dyke, situated at the limit between calc-alkaline and alkali-calcic suites; (2) the other dykes, which form a suite intermediate between alkaline and alkali-calcic suites.

The Vettaland samples have higher FeO*/MgO ratios than the Lomland samples (Fig. 2). Moreover, the Vettaland rocks are clustered in the AFM diagram while the Lomland dyke shows a trend of alkali enrichment accompanied by a slight FeO*/MgO increase when passing from the Puntervold to the Klungland facies. The other dykes roughly follow the Lomland linear trend. Plots of oxides against SiO_2, as exemplified by Fig. 3, also demonstrate the small variations in the Vettaland dyke, in contrast with the other dykes.

In the triangular diagram proposed by Philpotts (1981), monzonorites and (quartz) monzonites define a curve which might be interpreted as the boundary of an immiscibility field (Fig. 4). But because the Vettaland compositions plot inside this field, we believe that immiscibility does not play a significant role in the differentiation. The curve is the projection of the liquid line of descent in a process of fractional crystallization, which is demonstrated below.

Pertinent geochemical features of the trace element distribution are the following:

1. K/Rb values are high (1000–1400) in the monzonorites, and moderately high (600–800) in the monzonites and quartz monzonites (Vaersland). In the Vettaland dyke, the Eigeröy facies shows extreme values (5000). Sr is high in the Vettaland dyke (530–590 ppm); it slightly decreases from 460 to 390 ppm with increasing SiO_2 in the Lomland dyke. The K/Ba ratio appears rather constant in monzonorites (12–13) and increases slightly in monzonites and quartz-rich varieties (up to 21).

2. The Zr/Hf ratio shows its widest variation in the Lomland dyke (26–47). The Zr variation is the most significant in the Vettaland dyke where the Hetland facies is very rich (up to 1,400 ppm) while the Eigeröy facies is strongly depleted in Zr.

3. Most samples show chondrite-normalized values between 120 and 180 for the light REE (Fig. 5) and $[La/Yb]_N$ ratios
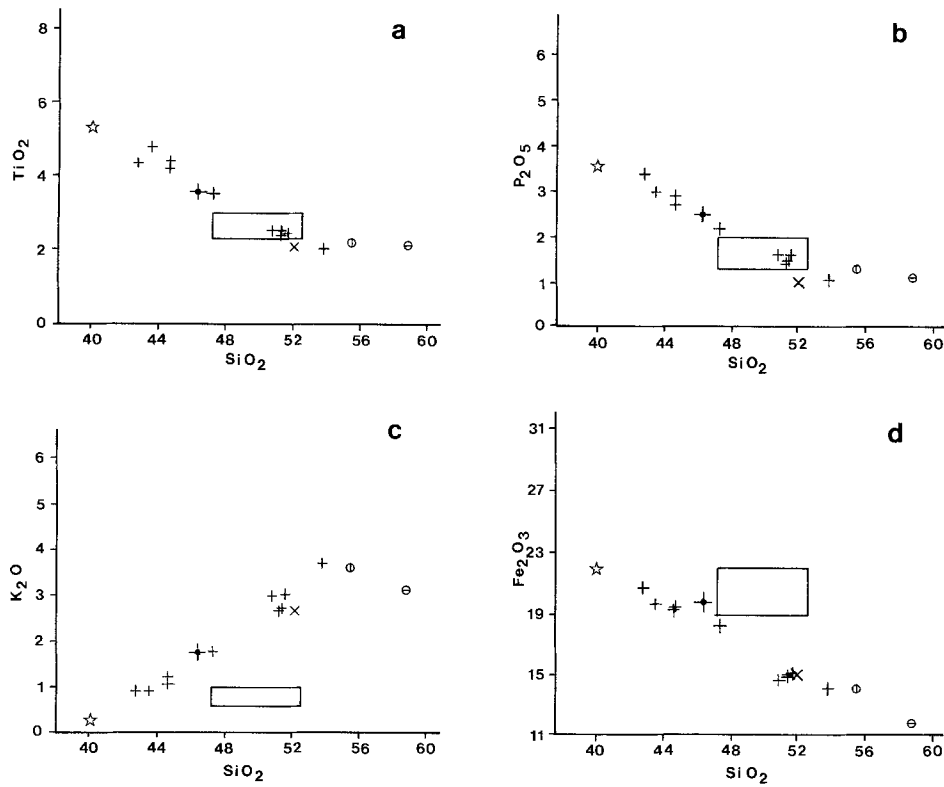
Fig. 3a–d. Plots of wt% SiO_2 against major oxides. Legend: same symbols as in Fig. 2; the Vettaland average composition plots in the middle of the rectangular area, the sides of which define the standard deviation of the averages ($\pm s$) (see Table 1); *open star*, Lomland calculated noritic cumulate (see Table 4)
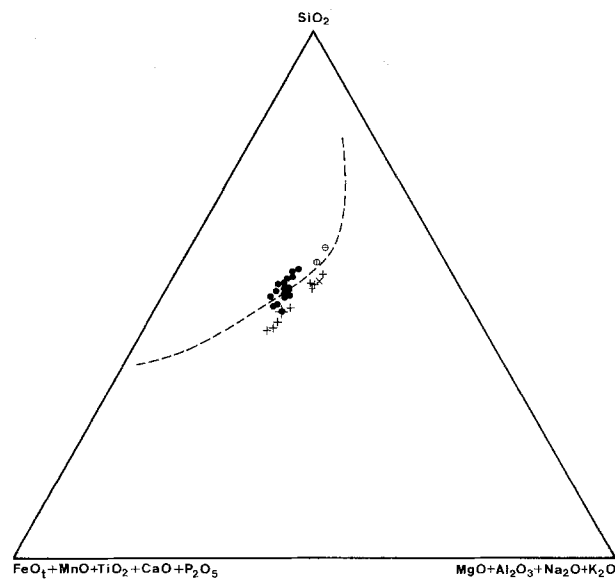

Fig. 4. $FeO^* + MnO + TiO_2 + CaO + P_2O_5$ – SiO_2 – $MgO + Al_2O_3 + Na_2O + K_2O$ triangular diagram (after Philpotts 1981). Same symbols as in Fig. 2. The *dashed line* represents the limit of the immiscibility field according to Philpotts

nearly constant (7 ± 2), except in the Eigeröy facies; the REE distributions usually display no Eu anomaly or a positive one; there is however a negative Eu anomaly in the most REE-rich samples (Sirevåg); a very peculiar REE distribution appears in the Eigeröy facies: low contents of the light and heavy REE, with enrichment in intermediate REE and a positive Eu anomaly.
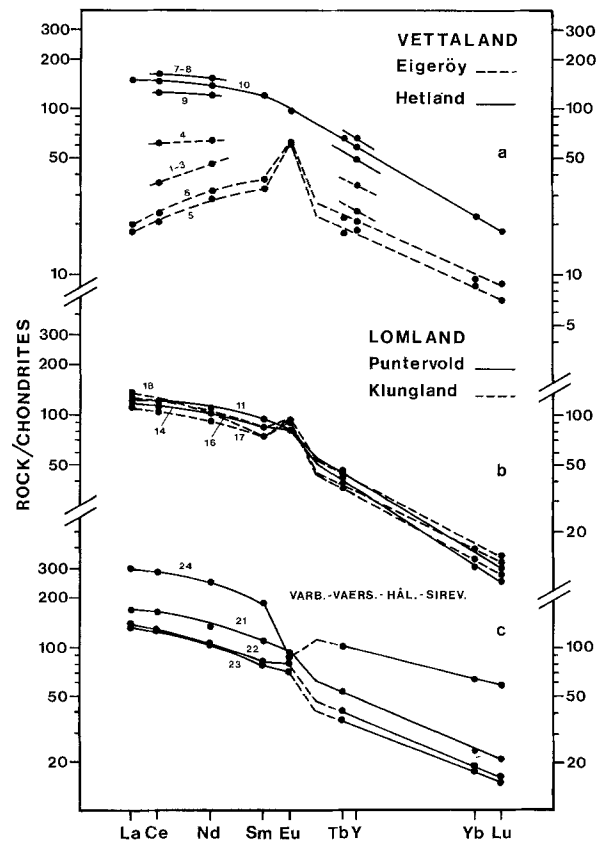

Fig. 5a–c. Chondrite-normalized REE distribution in the various occurrences (see Table 2). Note that in the Vettaland dyke, the yttrium values, normalized in order to fit the REE distribution, are also considered. Samples 1–4 were only analysed for Ce, Nd and Y by XRF (see Table 1). They give a good approximation of the REE distribution

4. As for the transition elements, Ni and Cr are very low (1–3 ppm and <10 ppm respectively); Sc (18–30 ppm) increases slightly with the mafic content; Co and Zn show small variations, while V significantly decreases with increase in SiO_2. No significant differences can be observed between the two Vettaland facies.

5. Th and U contents are very depleted, usually less than 0.5 ppm U and less than 1 ppm Th (except Sirevåg, with 2.1 ppm Th).

Role of apatite in the REE budget

The P_2O_5 contents and consequently the normative apatite content of the monzonorites are usually high (see Table 1). As apatite is usually rich in REE (Watson and Green 1981), it is interesting to examine the contribution of the apatite to the whole-rock REE budget. Apatites have therefore been separated from selected rocks and analysed for La. The results are reported in Table 3, together with data from Tables 1 and 2.

In the Lomland dyke the La content of the apatite is inversely correlated with the amounts of normative apatite, so that the contribution of the apatite to the La whole-rock content is virtually constant and equal to 60%–65%. This constancy suggests that the rocks simply result from the crystallization of magmatic liquids without any modification of the apatite proportions by cumulative processes or by separation of immiscible $P-Ti-Fe$-rich liquids in the course of crystallization. Apatite therefore appears not to be a cumulate phase in the Lomland dyke.

The Lomland dyke: evidence for fractional crystallization process

Major elements. In the AFM plot (Fig. 2) and in variation diagrams (Fig. 3), the samples from the Lomland dyke define linear evolution trends, passing from the Puntervold facies to the Klungland facies. Field evidence, lack of cumu-

Table 3. La content of apatites (ppm) and its contribution to the whole-rock La content

	Lomland				Vetta-land	Vaers-land
Rock no.	11	14	18	17	5	24
Specimen	66175	7534	7559	72105	7557	66192
La	376	419	841	736	115	878
%Ap[a]	7.5	6.3	3.1	3.3	3.0	2.8
La[b]	42.4	40.0	46.0	27.8	6.3	44.8

Apatite contribution to whole-rock La content

in ppm	28.2	26.4	26.1	24.3	3.45	24.6
in %	67	66	57	64	55	55

[a] Normative apatite content of the rock (see Table 1)
[b] Whole-rock La content (ppm)

late textures and REE content of apatite suggest that these rocks represent magmatic liquids.

The possibility of deriving the Klungland facies from the Puntervold facies by fractional crystallization and separation at depth of a "hidden" cumulate has been investigated. A least-square regression method (Table 4) has shown that, starting from the Puntervold average composition, subtraction of an oxide- and apatite-rich noritic cumulate gives a residual liquid close to the Klungland facies average composition, which therefore explains the major element variations in the dyke. The agreement between the calculated and observed values is excellent, the sum of squared residues (Σr^2) being 0.01.

Apatite can thus be considered a liquidus mineral for the Puntervold composition. As shown experimentally by Watson (1979), saturation in apatite depends on the P_2O_5 content of the magma as well as on the temperature and SiO_2 content. Watson's formula gives a temperature of 1,050° C for the Puntervold norite.

Table 4. Least-square fractionation model for the Lomland dyke

	Puntervold		Klungland[a]	Cumulate Comp.	Mineral composition used in fit[b]					
	Calc.	Obs.[a]			PLAG	OPX	CPX	ILM	MT	AP
SiO_2	43.43	43.45	51.46	39.92	59.00	48.02	50.43	–	1.19	–
TiO_2	4.41	4.41	2.41	5.25	–	0.15	0.49	50.60	10.75	–
Al_2O_3	12.80	12.76	14.63	11.99	26.00	2.15	2.33	–	2.07	
ΣFe_2O_3	19.61	19.61	14.64	21.67	–	33.24	12.62	48.14	85.99	–
MgO	3.96	3.90	2.26	4.66	–	16.12	12.88	1.26	–	–
CaO	8.68	8.67	6.20	9.71	7.60	0.22	20.73	–	–	56.79
Na_2O	3.24	3.23	3.97	2.92	6.70	0.10	0.53	–	–	–
K_2O	1.11	1.01	3.00	0.30	0.70	–	–	–	–	–
P_2O_5	2.95	2.96	1.44	3.58	–	–	–	–	–	43.21
Mineral proportions in cumulate (%)					42.68	21.71	8.28	7.85	11.20	8.28

$\Sigma r^2 = 0.0103$

Fraction of residual liquid after extraction of cumulate (F) = 0.298

All analyses (except the first column) recalculated to 100% after subtraction of MnO and with Fe as Fe_2O_3

[a] See Table 1
[b] The mineral compositions are close to those of the upper part of the anorthosito-noritic stage of the Bjerkreim-Sokndal lopolith (rhythm V in the stratigraphy of P. Michot 1960): PLAG (An_{37}); OPX ($Ca_{0.5}Fe_{49.9}Mg_{49.6}$); CPX ($Ca_{43}Fe_{19}Mg_{38}$) – from specimen JCD8027 (Duchesne, unpublished); ILM and MT from specimen JCD6482 (Duchesne 1972)

Table 5. Trace element modelling of the Lomland fractional crystallization

	Ck/Cp[a]	(S)[b]	D	Kd used in fit[c]
Ba	2.5	0.6	0.24	Kplag = 0.56
Rb	4.13	1.8	0	hygromagmaphile
Sr	0.86	0.15	1.12	Kplag = 2.4; Kap = 0.98[d]
Zn	0.92	0.1	1.07	Kmt = 9.5; Kilm = 0[e]
V	0.46	0.05	1.65	Kmt = 12; Kilm = 4[e]
Co	0.59	0.12	1.44	Kmt = Kilm = 7.5[e]
Sc	0.91	0.13	1.07	Kcpx = 3.8; Kopx = 1.6; Kilm = Kmt = 2.0[f]
Hf	3.67	1.05	0	hygromagmaphile
Zr	10	6	???	see text
La	1.10	0.13	0.92 ⎫	Kap = 12
Ce	0.92	0.10	1.07 ⎬	(average for La, Ce, Nd)[g]
Nd	0.93	0.12	1.06 ⎭	
Y	1.0	0.15		

Trace element contents in ppm, except REE contents, which are in chondrite-normalized values.

[a] From Table 1
[b] Standard deviation (S) calculated from the values in Table 1
[c] When the Kd value is not specified in a mineral, it is assumed to be equal to 0 for that mineral
[d] With Kap/plag = 0.41 (see Roelandts and Duchesne 1979)
[e] On the basis of the distribution between ilmenite and magnetite in coexisting pairs from the Bjerkreim-Sokndal lopolith (Duchesne 1972)
[f] Assuming Kcpx/opx = 2.3 and Kcpx/mt = 1.9 (see Schilling et al. 1978)
[g] It is assumed that the REE do not enter the other minerals

Trace elements. The results of the major element modelling can be extended to trace elements (Table 5). Assuming a Rayleigh fractional crystallization model, concentration of a trace element in Klungland (C_K) will be related to that in Puntervold (C_P) by the following equations:

$$C_K = C_P F^{D-1} \tag{1}$$

and

$$D = \Sigma \mu Kd \tag{2}$$

in which F is the fraction of liquid (= 0.298 – see Table 4), D the bulk partition coefficient, μ the mineral proportions in the cumulate (determined in Table 4) and Kd the solid/liquid partition coefficients. For hygromagmaphile elements (like Rb and Hf), D = 0 and Eq. (1) becomes $C_K/C_P = 1/F$ and the ratio C_K/C_P reaches its maximum value, 3.4 for F = 0.298.

Table 5 summarizes the evolution of the trace element contents between the two facies, of the bulk partition coefficients calculated from Eq. (1) and of the Kd values which fit the model. The latter are calculated using Eq. (2), which is greatly simplified in most cases because Kd values can be considered equal to zero in many minerals, the behaviour of a particular trace element being mainly controlled by one or two minerals.

Some points are worth commenting on

1). The apatite/liquid Kd for the REE – around 12 – is close to values used by Paster et al. (1974) to model the Skaergaard evolution and recommended by Hanson (1980) for basaltic compositions.

2. The evolution of Eu, which paradoxically shows an increase of its positive anomaly with differentiation (Fig. 5),

can be explained by subtraction of apatite (which has a negative Eu anomaly) together with plagioclase. The positive Eu anomaly of the plagioclase is outweighed by the negative anomaly of the apatite. In the present case, a simple calculation shows that a Kd of 9.0 for Eu in apatite fits the model, if we assume a Kd value of 0.40 for Eu in plagioclase (see Appendix 1 – Table 2), and a Kd of 13.4 for Eu* in apatite, a value consistent with the Kd of La, Ce and Nd. More elaborate calculations would require a better knowledge of the oxygen fugacity of the system. It is sufficient here to demonstrate that the evolution can be accounted for with plausible values of Kd.

3. Kd for transition elements are not well defined because their behaviour is controlled by several mafic minerals. For Zn, Co and V, additional constraints were defined from the data obtained on ilmenite-magnetite pairs in the Bjerkreim-Sokndal massif (Duchesne 1972). For Sc, values in agreement with those reviewed by Schilling et al. (1978) were obtained.

4. Ta, U and Th are not considered in Table 5. Ta and Th vary somewhat erratically and do not show the classical hygromagmaphile behaviour. U is also variable and depleted, as is common in rocks of the granulite facies.

5. Hf can be considered hygromagmaphile but Zr, in the Klungland facies, is much more enriched than should be expected if it is hygromagmaphile and shows a large scatter of values (s = 186 ppm, i.e. 32%). Actually the proposed model fails to explain the Zr behaviour in Lomland.

For most trace elements the partition coefficients which fit the model lie within the accepted limits of uncertainty. It can therefore be concluded that the behaviour of most trace elements does not contradict the fractional crystallization model developed for the major elements. The other monzonoritic occurrences show geochemical features broadly similar to those of Lomland. The Sirevåg dyke, however, is significantly enriched in REE and other hygromagmaphile elements and displays a negative Eu anomaly which requires a large amount of plagioclase fractionation.

The Vettaland dyke: evidence for eutectic partial melting

Regarding the major element contents, the Vettaland dyke rocks are very homogeneous (Figs. 2 and 3; Table 1): they could have been formed by crystallization of a single magmatic liquid. However, when trace elements are taken into consideration, the Hetland facies, comparable to common monzonorites in other dykes, appears quite distinct from the Eigerøy facies, which is depleted in LILE, and is characterized by an umbrella-shaped REE distribution with a positive Eu anomaly. Textural evidence suggests that the Eigerøy facies is not a cumulate rock and the chemical composition is not different from that of the Hetland facies, particularly in P_2O_5 and TiO_2.

The two facies could result from different degrees of partial fusion of the same source material. The constancy of the major element composition can be accounted for if the liquid is eutectic and remains at the eutectic during the melting process. Moreover, the Vettaland composition is very rich in Fe and plots in the AFM diagram (Fig. 2) not far from the Skaergaard late stage liquids [near the UZa liquid of Wager and Brown (1968), corresponding to 96% solidification]. If partial fusion is considered an equi-
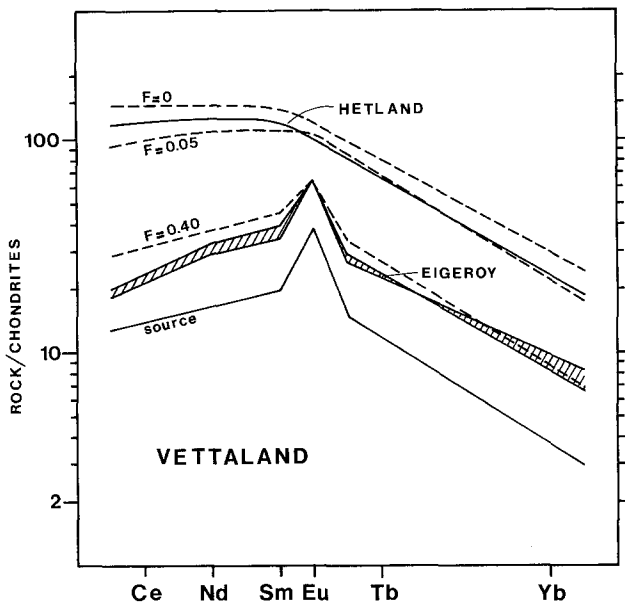
Fig. 6. Comparison of the measured REE distributions in the Vettaland dyke with those calculated from a partial melting model (see text). The Kd values used for apatite are: Ce = 4.5, Sm = 7.0, Eu = 6.0, Tb = 7.0, and Yb = 4.0. Various degrees of partial melting (F = 0, 0.05, 0.40) of the source rock are represented by the dashed lines (see text). They are compared to the Hetland and Eigeröy facies

librium process, the composition of the starting material must not be very different from that of the liquid. Therefore, the source rock must be a moderately Fe-enriched gabbro or norite.

Fusion of a basic rock to produce an iron-rich and relatively SiO_2-poor liquid of monzonoritic composition requires the same physicochemical conditions as those which control the formation of Fe-enriched liquids through fractional crystallization, that is, low water content and low fO_2, as well as moderate depths. By contrast, dacitic liquids would be produced in wet conditions with an amphibolite residue (Helz 1976) or at greater depths with an eclogite residue (Green and Ringwood, 1967). The anorthositic plutonism provides a suitable environment for the development of such a dry basic anatexis: indeed, anorthosite emplacement as hot diapirs of rising plagioclase crystal mush (Maquil and Duchesne 1984) in the granulite facies lower crust could induce this anatexis.

The model. By trial and error, the composition of a possible source rock for the Vettaland liquids has been found to be a basic rock containing 1.5% apatite and characterized by a positive Eu anomaly and a somewhat depleted light REE distribution, as shown in Fig. 6. Such a REE distribution can be accounted for by various mineral associations provided it contains suitable amounts of plagioclase (positive Eu anomaly) and apatite (light REE depletion). The latter mineral plays a critical role, since it is present in minor amounts (1.5%) but provides a large part of the REE content of the rock (e.g. up to 80% of the Sm content).

Besides the apatite content, the following mineral content for the source rock has been assumed: 45% plag(An_{40}) + 22% opx + 9% cpx + 12% ilm + 10% mag. Such an association is commonly found in norite cumulates, e.g. in Bjerkreim-Sokndal (see Duchesne 1978), and has a major

element composition not far from that of the Vettaland composition.

The mathematical expression of the model is equilibrium non-modal melting

$$C_L/Co = 1/Do + F(1 - P) \qquad (3)$$

where C_L and Co are the concentrations of a given element in the liquid and in the initial solid, respectively, F is the fraction of melt, Do is the bulk partition coefficient at the beginning of melting and P is the bulk partition coefficient for the melt proportions.

The Kd values used in the calculations of Do and P (Appendix 1) have been determined on the basis of the composition of the various minerals of a noritic cumulate of the Bjerkreim-Sokndal massif (Duchesne 1978; Roelandts and Duchesne 1979). The silicate minerals Kd values are interestingly close to those calculated by Paster et al. (1974) for the Skaergaard differentiation. For apatite the Kd's used are 2 times lower than those which fit the Lomland crystallization model (Table 4). Watson and Green (1981) have shown on experimental grounds that apatite/melt Kd values are very sensitive to temperature and SiO_2 content of the melt and particularly that a two-fold decrease in the values can be due to a 130° C increase in temperature. The difference between the Lomland and Vettaland magmas, both in temperature and composition, can account for the variation in the apatite Kd values. The mineral proportions used in calculation of Do and P are respectively those assumed for the source and those calculated from the average normative composition of the Vettaland dyke (Table 1). Equation (3) is used until the total exhaustion of apatite, which takes place for F = 0.40. Figure 6 shows that the model satisfactorily accounts for the Hetland facies (0–5% partial melting) and for the Eigeröy facies (up to 40% partial melting).

The behaviour of the other trace elements can also be understood in the light of the model. The strong depletion of Zr in the Eigeröy facies indicates that trace amounts of a Zr-bearing mineral, initially present in the source rock, are used up in the first stages of the melting process and that no Zr is left in the source rock for higher F values. On the other hand, the relatively slight variations of Sr and transition elements between the two facies are due to the small variations in the main mineral proportions in the source rocks during the process, as can be forseen on the basis of the similarity between the major element compositions of the source rock and the melt.

In conclusion, the geochemical characters of the Vettaland dyke – constancy of major elements and strong variation in trace elements – can be explained by partial melting of a basic cumulate rock under granulite facies conditions.

Sr and Pb isotopic compositions

The measured Sr isotopic ratios on selected samples are plotted in Fig. 7 (see Table 6). The Lomland samples are roughly aligned (except sample 19[2]) around a 950 Ma refer-

2 Sample 19 comes from a thin (10 cm) dyke a few tens of metres from the main Lomland dyke. Its overall petrographic and chemical characteristics point to a close relation with Lomland, and explain that it has not been distinguished from it in the previous sections. Nevertheless, the Sr isotopic composition indicates that the relation is more complex
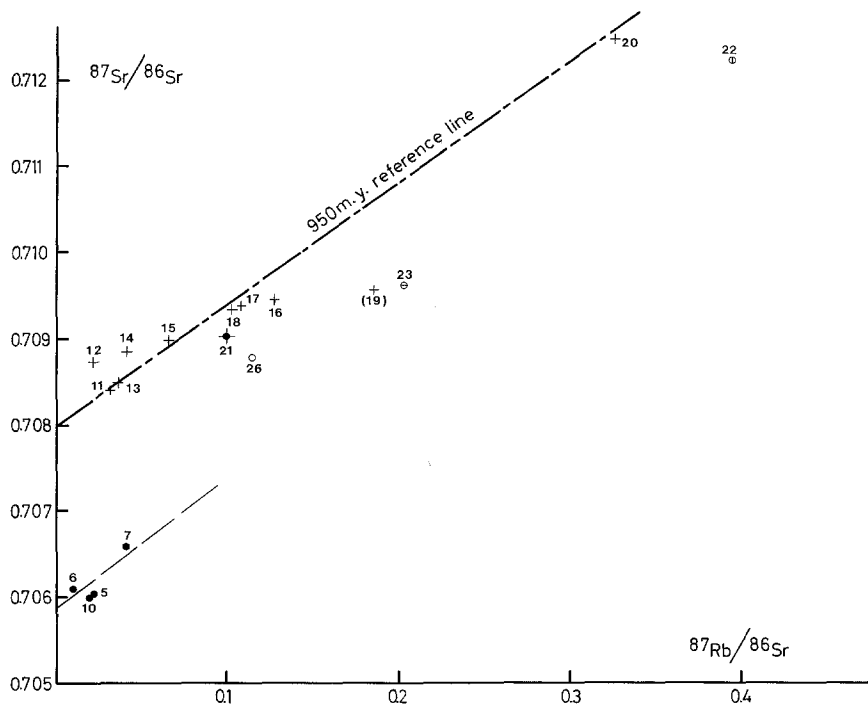
Fig. 7. $^{87}Sr/^{86}Sr$ versus $^{87}Rb/^{86}Sr$ diagram for various monzonorites. Same symbols as in Fig. 2; the numbers refer to Table 1

Table 6. Rb and Sr analytical data

Sample	Rb ppm	Sr ppm	$^{87}Rb/^{86}Sr$	$^{87}Sr/^{86}Sr$	$2\sigma_n$ $(\times 10^{-5})$
Vettaland					
5 (7557)	4.3*	571	0.0218	0.70604	3
6 (7522)	2.0*	529	0.0108	0.70609	10
7 (7527)	6.9*	489	0.0408	0.70662	4
10 (7529)	3.9*	607	0.0186	0.70601	5
Lomland					
11 (66175)	5.1*	438*	0.0338	0.70840	11
12 (7536)	3.7*	485*	0.0221	0.70875	5
13 (7553)	5.6*	436*	0.0372	0.70851	3
14 (7534)	6.9*	473*	0.0423	0.70887	3
15 (7553)	9.7*	417*	0.0673	0.70898	3
16 (7552)	20.1*	452*	0.1289	0.70947	2
17 (72105)	16.9*	447	0.1095	0.70939	5
18 (7559)	15	411	0.1057	0.70936	12
19 (7365)	22.3*	347	0.1861	0.70956	4
20 (8147)	35.2*	310	0.3288	0.71272	6
Varberg					
21 (7520)	13.9	406	0.0992	0.70906	18
Vaersland					
22 (66192)	40	294	0.3944	0.71226	15
Håland					
23 (7548)	23.5	335	0.2032	0.700965	4

Rb and Sr determined by XRF (analysts C. Léger and A. Kool, MRAC, Tervuren, Belgium), except the values marked by *, which were determined by isotopic dilution

ence line corresponding to the crystallization age of the monzonoritic dykes (U−Pb zircon data: Pasteels et al. 1979), which gives a Sr isotopic initial ratio (I_{Sr}) close to 0.7080. The four analysed samples of the Vettaland dyke have distinctly lower Sr ratios of about 0.7060, very close

to the initial Sr isotopic composition since the $^{87}Rb/^{86}Sr$ ratios are less than 0.04. The Varberg dyke data point (no. 21) is close to the Lomland 950 Ma reference line. The other samples (Vaersland, Håland, no. 19) plot below it.

The Pb isotopic compositions for some of the monzonoritic dykes are shown in Fig. 8. The Lomland dyke samples have very comparable Pb isotopic compositions, with a relatively small scatter of values: 17.96 to 18.55 for the $^{206}Pb/^{204}Pb$ ratios and 15.55 to 15.60 for the $^{207}Pb/^{204}Pb$ ratios. The samples from Varberg (no. 21) and Vaersland (no. 22) have Pb isotopic ratios not very different from those of the Lomland dyke. The Vettaland dyke has well-scattered Pb isotopic ratios, shown by samples 5 and 10, which for the same $^{206}Pb/^{204}Pb$ values of 17.9, have $^{207}Pb/^{204}Pb$ ratios of 15.58 and 15.54 respectively. Moreover, samples 5 and 6, which belong to the Eigeröy facies, are distinctly lower in U and Th than samples 7 and 10 of the Hetland facies. The same kind of grouping is observed in the $^{208}Pb/^{204}Pb$ versus $^{206}Pb/^{204}Pb$ diagram.

In Fig. 8 the Lomland dyke data roughly define a linear array, the slope of which roughly corresponds to 950 Ma. When corrected for the in situ U decay for 950 Ma, the three samples for which U and Pb contents are available give similar "initial" Pb ratios (point L on Fig. 8).

Discussion

The Sr isotopic data show that each monzonoritic dyke is distinct but that, within a dyke, there is no isotopic variation. The enclosing anorthositic massifs also display variable I_{Sr}, as shown by Demaiffe (1977) and Duchesne and Demaiffe (1978): Egersund-Ogna (0.7035–0.7045); Håland-Helleren (0.705–0.706); Bjerkreim-Sokndal anorthosites and norites (ca. 0.7057). This precludes any direct relation of any of these massifs with the Lomland dyke, which has a higher I_{Sr}. Regarding the Vettaland dyke, its I_{Sr} (ca. 0.706) is not far from Bjerkreim-Sokndal, but quite distinct from the enclosing Egersund-Ogna massif.

Table 7. Pb isotopic compositions

Sample	$^{206}Pb/^{204}Pb$[a]	$^{207}Pb/^{204}Pb$	$^{208}Pb/^{204}Pb$	Pb[b]	U[b]	Th[c]	$^{238}U/^{204}Pb$
Vettaland							
5 (7557)	17.901	15.580	37.068		0.11[c]	<0.2	
6 (7522)	18.955	15.626	37.228		<0.1[c]	<0.1	
	18.965	15.650	37.274				
7 (7527)	18.229	15.560	37.083	4.65	0.38		5.057
10 (7529)	17.909	15.536	37.142	4.45	0.23–0.26[c]	0.30	3.188
Lomland							
11 (66175)	18.553	15.595	37.689	3.14	0.30–0.31[c]	0.71	6.047
15 (7553)	18.102	15.562	37.344	5.33	0.26		3.029
	18.096	15.558	37.314				
19 (7365)	17.956	15.546	37.215	6.10	0.22		2.182
20 (8147)	18.036	15.549	37.295				
Varberg							
21 (7520)	18.109	15.559	37.354		0.30[c]	0.59	
	18.048	15.535	37.514				
Vaersland							
22 (66192)	17.800	15.538	37.184		0.20[c]	0.20	

[a] Results corrected for mass discrimination ($1.34 \pm 0.4\%$, a.m.u) on the basis of repeated analyses of the NBS 981 Pb standard
[b] In ppm – isotope dilution mass spectrometry
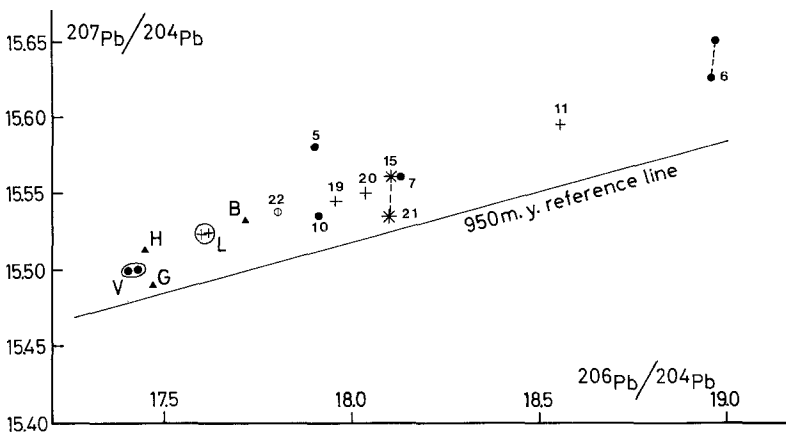[c] In ppm – instrumental neutron activation analysis

Fig. 8. $^{207}Pb/^{204}Pb$ versus $^{206}Pb/^{204}Pb$ diagram. Same symbols as in Fig. 2; the numbers refer to Table 1. L and V indicate the initial ratios for the Lomland and Vettaland dykes respectively. B, H and G correspond to the initial ratios of the Bjerkreim-Sokndal acidic rocks, of the Hidra charnockitic dykes, and of the average granulite facies gneisses, respectively (see text)

The high I_{Sr} ratios also indicate that monzonorites are not directly derived from a mantle source. The hypothesis of Emslie (1978) – derivation from a tholeiitic basaltic magma – thus cannot be generalized to all occurrences.

Depletion in Rb and U due to a granulite facies metamorphism (see Heier 1973) occurring after the crystallization of the dykes must be rejected. The dykes indeed intruded after the regional deformation, and mostly display a typical magmatic texture with no indication of a metamorphic overprint.

Charnockitic acid rocks associated with the anorthosites usually present Sr and Pb characteristics, indicating either a large amount of contamination by crustal material or direct melting from lower crustal source rocks (Demaiffe et al. 1979; Weis and Demaiffe 1983a). The high I_{Sr} values of the Lomland dyke (ca. 0.708) as well as the position of the Pb initial ratio (point L, Fig. 8), intermediate between the Hidra charnockitic dykes (point H) and the Bjerkreim-Sokndal acidic rocks (point B), can be explained by a con-

tamination process but cannot preclude direct melting of lower crustal material. The low U content of Lomland (<0.3 ppm) together with the high I_{Sr} indicate that the contaminant or the source rock were relatively more depleted in U than in Rb, a fact already observed in many granulite facies domains (Ben Othman et al. 1984).

The initial Pb ratios for the Hetland facies of the Vettaland dyke (point V on Fig. 8) plot near the Rogaland average granulite material (point G, Fig. 8) (Weis and Demaiffe 1983b). This again points to strong contamination or direct melting.

Our geochemical data, however, suggest that partial melting can be preferred to all other processes to account for the monzonorites. We have indeed shown that a ferronoritic cumulate can be the source rock of the Vettaland dyke. Because of the many similarities of part of the dyke (the Hetland facies) with common monzonorites, the partial melting hypothesis can be extended to all occurrences. The low level of U and Th and the range of values of the I_{Sr}

(0.706–0.708) indicate that the source rock was in the granulite facies and the K_2O content points to a basic to intermediate composition.

Conclusions

The geochemical features of the monzonoritic liquids (no Eu anomaly, high Sr initial ratios, Pb isotopic composition) suggest that they are not strictly comagmatic with massif-type anorthosites and that they are not generated in the upper mantle.

Fractional crystallization by subtraction of a noritic cumulate can explain the variety of rocks from norite to (quartz) monzonite. This shows that monzonoritic magmatism can give rise to acidic rocks without any contamination during the process (constant initial Sr and Pb ratios in the Lomland dyke).

The Vettaland dyke is a remarkable case of eutectic partial melting, the source rock being an apatite-bearing ferronoritic cumulate. The process would have taken place in a granulite facies environment (low pH_2O) in moderate total pressure conditions (plagioclase is stable in the residue). The necessary heat of melting might have been provided by the huge diapirs of anorthositic mush which constitute the massif anorthosites.

In view of the similarities between part of the Vettaland dyke and other monzonorites, it is suggested that the partial melting process of granulite facies rocks could be generally applied to account for all monzonoritic occurrences, rather than advocating variable crustal contamination of mantle-derived liquids.

Appendix 1

Table 1. REE content (ppm) in the various cumulate minerals of a norite from the Bjerkreim-Sokndal lopolith (rock specimen JCD6444)

	La	Ce	Nd	Sm	Eu	Tb	Yb	Lu
Apatite[a]	216	606	479	130	25.9	16.1	17.8	1.9
Plagioclase[a]	2.98	4.94	2.1	0.33	1.66	0.034	0.043	0.007
Orthopyroxene	0.49	1.85	1.3	0.41	0.10	0.084	0.49	0.10
Clinopyroxene	3.04	12.6	14.6	6.05	1.52	1.03	1.61	0.26
Ilmenite	0.74	1.81	0.9	0.29	0.092	0.033	0.14	0.033
Magnetite	0.27	0.74	0.5	0.10	0.03	0.013	0.036	0.005

[a] See Roelandts and Duchesne (1979)

Table 2. Mineral/melt distribution coefficients for the REE used in modelling the Bjerkreim-Sokndal differentiation

	La	Ce	Nd	Sm	Eu	Tb	Yb	Lu
Apatite[a]	4.3	5.5	6.9	7.3	5.8	7.7	4.05	3.3
Plagioclase[b]	0.053	0.040	0.022	0.014	0.27–0.63[c]	0.010	0.007	0.0065
Orthopyroxene	0.012	0.015	0.019	0.022	0.023	0.036	0.111	0.156
Clinopyroxene	0.06	0.11	0.21	0.34	0.34	0.44	0.40	0.41
Ilmenite	0.015	0.016	0.017	0.018	0.018	0.019	0.034	0.040
Magnetite	0.006	0.006	0.006	0.006	0.006	0.006	0.008	0.009

[a] From Roelandts and Duchesne 1979; Duchesne 1978
[b] Calculated on the basis of the distribution between 7 pairs of plagioclase and apatite (Roelandts and Duchesne 1979)
[c] K_{Eu}^{plag} depends on oxygen fugacity (see Table 4 in Roelandts and Duchesne 1979)

Appendix 2. Analytical procedures

Major elements were determined by X-ray fluorescence on a CGR Lambda 2020 spectrometer on Li borate glass discs. The trace elements reported in Table 1 were also measured by XRF, matrix corrections being calculated from the major element composition. FeO was measured by titration.

Neutron-activation analyses have been carried out at the Mineralogisk-Geologisk Museum, Oslo University, Norway. USGS reference basalt BCR-1 was used as a multi-element standard. Details have been reported previously (Roelandts 1975, 1977). Results reported in Tables 1 and 2 are averages of 2–5 replicate analyses. The relative standard deviations were as follows: La 2.4%; Ce 4.4%; Nd 7.8%; Sm 2.7%; Eu 6.5%; Tb 7.1%; Yb 8.9%; Lu 6.8%; Ba 4.6%; Co 5.8%; Cr 5.0%; Hf 10%; Rb 5.4%; Sc 7.8%; Sr 7.9%; Ta 9.8%; Th 25%; U 45%. Our values on geochemical reference samples are in close agreement with the "consensus values" of Gladney et al. (1983). Some light REE have been determined in apatites by XRF after anion exchange extraction (Roelandts 1981).

Rb, Sr, U and Pb concentrations were determined in some samples by isotope dilution mass spectrometry on a VARIAN TH5 mass spectrometer. Sr was separated in an ion-exchange column and its isotopic composition was measured by thermoionization with a double rhenium filament on a FINNIGAN MAT 260 mass spectrometer. The $^{87}Sr/^{86}Sr$ values were normalized to $^{88}Sr/^{86}Sr = 8.3752$. Ten determinations of the Eimer and Amend Sr standard yielded an average $^{87}Sr/^{86}Sr$ ratio of 0.70807 ± 7. Pb was separated with an ion-exchange column in a HBr-HCl medium and loaded on a single rhenium filament using the silica gel/H_3PO_4 method (see Weis 1981, for detailed procedure). The Pb isotopic composition measured on a FINNIGAN-MAT260 mass spectrometer was corrected for mass discrimination ($1.34 \pm 0.4\%$, per a.m.u.) on the basis of 25 analyses of the NBS 981 Pb standard. All blanks were less than 2 ng Pb.

References

Ashwal LD (1982) Mineralogy of mafic and Fe−Ti oxide rich differentiates of the Marcy anorthosite massif, Adirondacks, New York. Am Mineral 67:14–27

Ben Othman D, Polvé M, Allègre CJ (1984) Nd−Sr composition of granulites. Constraints on the evolution of the lower continental crust. Nature 307:510–515

Buddington AF (1972) Differentiation trends and parental magmas for anorthositic and quartz mangerite series, Adirondacks, New-York. Geol Soc Am Mem 132:477–488

Demaiffe D (1977) De l'origine des anorthosites. Pétrologie, géochimie et géochimie isotopique des massifs anorthositiques de Hidra et de Garsaknatt (Rogaland, Norvège méridionale). Unpubl Dr Sc Thesis, Univ Bruxelles

Demaiffe D, Hertogen J (1981) Rare earth geochemistry and strontium isotopic composition of a massif-type anorthositic-charnockitic body: the Hidra massif (Rogaland, S.W. Norway). Geochim Cosmochim Acta 45:1545–1561

Demaiffe D, Duchesne JC, Hertogen J (1979) Trace element variations and isotopic composition of charnockitic acidic rocks related to anorthosites (Rogaland – S.W. Norway). In: Ahrens LH (ed) Origin and distribution of the elements. Pergamon Press, pp 417–429

Demaiffe D, Michot J (1985) Isotope geochronology of the Proterozoic crustal segment of Southern Norway: a review. In: Touret J (ed) "The deep Proterozoic crust in the North Atlantic Provinces". Reidel (in press)

Duchesne JC (1972) Iron-Titanium oxide minerals in the Bjerkrem-Sogndal massif, Southwestern Norway. J Petrol 13:57–81

Duchesne JC (1978) Quantitative modeling of Sr, Ca, Rb and K in the Bjerkrem-Sogndal layered lopolith (S.W. Norway). Contrib Mineral Petrol 66:175–184

Duchesne JC, Demaiffe D (1978) Trace elements and anorthosite genesis. Earth Planet Sci Lett 38:249–272

Duchesne JC, Demaiffe D, Maquil R, Michot J, Wilmart E (1984) The Rogaland intrusive masses. In: Excursion guide of the South Norway geological excursion", NATO Adv Stud Inst Moi, July 1984

Duchesne JC, Roelandts I, Demaiffe D, Hertogen J, Gijbels R, De Winter J (1974) Rare-earth data on monzonoritic rocks related to anorthosites and their bearing on the nature of the parental magma of the anorthositic suite. Earth Planet Sci Lett 24:325–335

Emslie RF (1978) Anorthosite massifs, Rapakivi granites, and late Proterozoic rifting of North America. Precamb Res 7:61–98

Gladney ES, Burns CE, Roelandts I (1983) 1982 compilation of elemental concentrations in 11 US Geological Survey rock standards. Geostand Newsl 7:3–226

Green DH, Ringwood AE (1967) The genesis of basaltic magmas. Contrib Mineral Petrol 15:103–190

Hanson G (1980) Rare earth elements in petrogenetic studies of igneous systems. Ann Rev Earth Planet Sci 8:371–406

Heier KS (1973) Geochemistry of granulite facies rocks and the problems of their origin. Phil Trans Roy Soc London A273:429–442

Helz RT (1976) Phase relations of basalts in their melting ranges at $PH_2O=5\,Kb$. Part II. Melt compositions. J Petrol 17:139–193

Maquil R, Duchesne JC (1984) Géothermométrie par les pyroxènes et mise en place du massif anorthositique d'Egersund-Ogna (Rogaland, Norvège méridionale). Ann Soc Géol Belg 107:27–49

Michot P (1960) La géologie de la catazone: Le problème des anorthosites, la palingenèse basique et la tectonique catazonale dans le Rogaland méridional (Norvège méridionale). Norges Geol Unders 212g:1–54

Michot P (1965) Le magma plagioclasique. Geol Rundschau 54:956–976

Michot J, Michot P (1969) The problem of the anorthosites. The South Rogaland igneous complex (South Western Norway). In: Isachsen YW (ed) "Origin of anorthosites and related rocks", N Y State Mus Sci Serv Mem 18:399–410

Pasteels P, Demaiffe D, Michot J (1979) U−Pb and Rb−Sr geochronology of the eastern part of the South Rogaland igneous complex, Southern Norway. Lithos 12:199–208

Paster TP, Shauwecker DS, Haskin LA (1974) The behaviour of some trace elements during solidification of the Skaergaard layered series. Geochim Cosmochim Acta 38:1549–1577

Philpotts AR (1966) Origin of the Anorthosite-Mangerite rocks in Southern Quebec. J Petrol 7:1–64

Philpotts AR (1981) A model for the generation of massif-type anorthosites. Can Mineral 19:233–253

Roelandts I (1975) Contribution au dosage par activation neutronique des terres rares et d'autres éléments en trace dans les roches magmatiques. Unpubl Dr Sc Thesis, Univ Liège

Roelandts I (1977) Silicate rock and rock-forming mineral neutron activation analysis. Radiochim Acta 24:139–146

Roelandts I (1981) Determination of light rare earth elements in apatite by X-ray fluorescence spectrometry after anion exchange extraction. Anal Chem 53:676–680

Roelandts I, Duchesne JC (1979) Rare-earth elements in apatite from layered norites and iron-titanium oxide ore-bodies related to anorthosites (Rogaland, S.W. Norway). In: Ahrens LH (ed) Origin and distribution of the elements. Pergamon, pp 199–212

Schilling JG, Sigurdsson H, Kingsley RH (1978) Skagi and Western Neovolcanic zones in Iceland: 2. Geochemical variations. J Geophys Res 83:3983–4002

Wager LR, Brown GM (1968) Layered igneous rocks. Oliver and Boyd Ltd, London

Watson EB (1979) Apatite saturation in basic to intermediate magmas. Geophys Res Lett 6:939–940

Watson EB, Green TH (1981) Apatite/liquid partition coefficients for the Rare Earth elements and Strontium. Earth Planet. Sci Lett 56:405–421

Weis D (1981) Composition isotopique du plomb total de roches: méthodologie. Bull Soc Chim Belg 90:1127–1140

Weis D, Demaiffe D (1983a) Pb isotope geochemistry of a massif-type anorthositic body: the Hidra massif (Rogaland, S.W. Norway). Geochim Cosmochim Acta 47:1405–1413

Weis D, Demaiffe D (1983b) Age relationships in the Proterozoic high-grade gneiss of Southern Norway: discussion and comment. Precamb Res 22:149–155

Wiebe RA (1984) Fractionation and magma mixing in the Bjerkrem-Sogndal lopolith (S.W. Norway): evidence for the compositions of residual liquids. Lithos 17:171–188